A Hybrid Deep Learning Approach for Coronary Artery Disease Detection and Severity Analysis Using ECG Signals

Kushwant Kaur
Department of Computer Science and Engineering, Chandigarh University, Mohali, India
khushi.rai1@gmail.com (corresponding author)

Gaurav Bathla
Department of Computer Science and Engineering, Chandigarh University, Mohali, India
gaurav.bathla@gmail.com

Received: 1 July 2025 | Revised: 28 July 2025 | Accepted: 15 August 2025

 DOI: https://doi.org/10.48084/etasr.13103

ABSTRACT

Cardiovascular diseases such as Coronary Artery Disease (CAD) are life-threatening. CAD can be detected in the early stages using Electrocardiogram (ECG) signals. However, ECG disturbances have a wide range of manifestations with varying clinical significance. This paper presents a deep learning-based technique for the detection of CAD using ECG signals. The proposed method addresses common signal quality issues by employing advanced preprocessing techniques, including elliptic (Cauer) filtering for baseline wander elimination, Chebyshev Type I filtering for power line interference removal, and adaptive comb filtering for electrode motion artifacts exclusion. The preprocessed signals are then standardized using z-score normalization. During signal segmentation (one beat in each segment), the proposed model eliminates false peaks based on an adaptive threshold with morphological and statistical evaluation. The proposed model integrates Bidirectional Long Short-Term Memory (Bi-LSTM) and Neural Basis Expansion Analysis for Time Series (N-BEATS) for feature extraction, dimensionality reduction, and classification. A clustering approach is used to not only enhance the accuracy of cluster formation but also improve the overall efficiency of the K-means algorithm. By integrating the dynamic characteristics of horse herd behavior, the method adapts to varying data distributions, leading to more robust clustering results. After CAD detection, its severity is categorized using the Minnesota Code (MC) by analyzing QRS voltage, ST elevation, ST depression, and T-wave inversion patterns on different ECG leads. The proposed system was evaluated using accuracy, specificity, sensitivity, and F1-score, showing that it has the potential to aid clinicians in the detection of CAD in the initial stages using ECG signals.

Keywords-coronary artery disease; ECG signal; segmentation; deep learning; feature extraction; baseline wander

I. INTRODUCTION

Stressful workloads, lifestyle changes, hectic paces, and unbalanced food habits are the main causes of heart disease [1]. According to World Health Organization (WHO) statistics, approximately 17.9 million people die from Cardiovascular Diseases (CVD) each year. The key source of CVD is atherosclerosis, which arises due to the obstruction of blood vessels by the formation of plaque on the walls of the inner layer of the arteries. Plaque is formed by the deposition of fatty materials, calcium, cellular waste, cholesterol, and fibrin [2]. In Coronary Artery Disease (CAD), oxygen-rich blood flows along plaques in the arteries, and breakage of this plaque causes blood clots that trigger thrombosis, resulting in myocardial infarction [3]. In addition, stenosis reduces or blocks the blood supply to the heart, leading to angina pectoris [4].

An electrocardiogram (ECG) test is a non-invasive procedure in which doctors attach various sensors to different parts of the body, including the arms, legs, and especially the chest. Some typical changes in ECG signals are associated with some specific diseases, such as CAD; therefore, the ECG provides a wide source of useful information to diagnose and predict CVD. CAD generally appears in an ECG with a downward displacement of the S Transformation (ST) segment or a short period of elevation [5]. ECG signals have been widely applied to diagnose heart diseases, such as arrhythmia and myocardial infarction [6]. Morphological changes in the ECG signal, such as elevation of the ST-segment and inversion or flatness of the T-waves, are indicative of manifestations of myocardial ischemia or infarction resulting from CAD [7].

In most cases, traditional rule-based diagnosis is inefficient when dealing with large amounts of various information and

requires substantial evaluation and medical knowledge to ensure tolerable accuracy in the evaluation [8]. Invasive angiography is the gold standard diagnosis for CAD, but requires admission to the hospital. Early detection of the disease can usually avoid the fatal penalties of the most dangerous CVDs [9]. The key mechanisms for the identification and resolution of CVD include beat extraction and classification. For example, various people suffer from detrimental heart pulses that are fatal in certain cases. Therefore, it is necessary to detect hypertrophic heart rates accurately and economically [10]. Deep Learning (DL) algorithms can be implemented to design automated systems for accurate and fast diagnosis. The Internet of Things (IoT) is causing a slow transformation in the health industry, with the aim of making it easier for patients to submit health information and get prescriptions from doctors online [11].

This study aimed to detect and classify the severity of CAD with high accuracy using ECG signals, based on a hybrid DL approach. The proposed method ensures data quality by removing various artifacts from the signals, such as baseline wander, powerline interference, and electrode motion artifacts [12]. An elliptic filter was used to remove baseline wander, a Chebyshev type I filter was used to remove powerline interference, and an adaptive comb filter was used to remove electrode motion artifacts. After denoising the signals to extract effective features, segmentation was performed using improved linear regression, and elimination of false peaks was performed to reduce high false positive rates. Finally, to improve classification accuracy, a hybrid DL algorithm was implemented to extract optimal features, and clustering was performed using K-Means based on the Horse herd Optimization Algorithm (HOA). Then, a classification was performed to identify the severity level of CAD.

II. METHODOLOGY

The proposed method aims at the accurate detection of CAD using ECG signals. In addition, the severity level of CAD is detected accurately by extracting effective features. The detection accuracy of the model is improved using preprocessing, segmentation, and feature extraction [13]. The proposed method involves three consecutive processes:

- Signal Quality Evaluation,
- False Peak Elimination and Signal Segmentation,
- Hybrid Feature Extraction and Classification.

A. Signal Quality Evaluation

Although modern ECG devices incorporate advanced filtering techniques, signal artifacts, such as baseline wander, power-line interference, and motion artifacts, can still affect signal quality—particularly in ambulatory, wearable, or resource-limited settings. Therefore, signal preprocessing remains essential to ensure reliable analysis. Figure 1 describes the process of evaluating signal quality. Table I describes the filters used in the process of eliminating artifacts from signals.

TABLE I. FILTERS FOR ARTIFACTS ELIMINATION

Type of filter	Artifacts/ Noise	Use	Characteristics
Elliptic filter (Cauer filter)	Baseline wander	Eliminate low-frequency baseline wander noise	Ensures the equiripple behavior in the passband and stopband
Chebyshev Type I filter	Power-line interference	Remove power-line interference (50/60 Hz) without greatly impacting the ECG signal	Offers a sharper roll-off compared to Butterworth filters
Adaptive Comb filter	Electrode motion artifact	Eliminate periodic noise by focusing on its harmonic frequencies	Ensures stability due to the linear phase

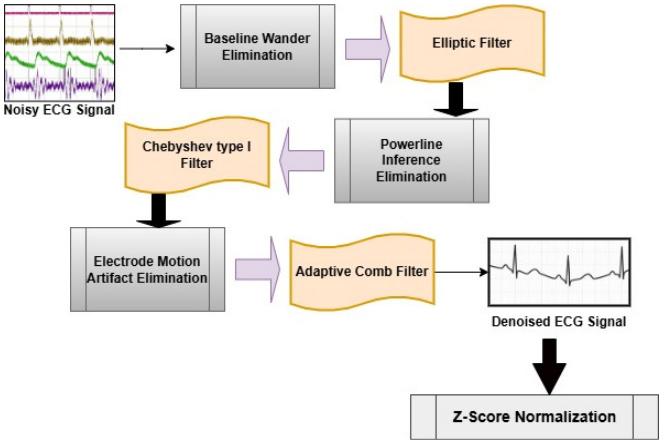

Fig. 1. Signal quality evaluation.

1) Elimination of Baseline Wander

ECG signals have a low-frequency artifact known as baseline wander that makes their interpretation difficult. The elimination of baseline wander is a significant preprocessing step to improve signal quality. For this purpose, an elliptic filter (Cauer filter) was used to achieve a sharper cut-off by behaving in both the passband and stopband. The amplitude response of the filter is represented by:

$$|A(\vartheta)| = \frac{1}{\sqrt{1+\varepsilon^2 B_n^2\left(\vartheta/\vartheta_d\right)}} \quad (1)$$

where ε represents the ripple factor, ϑ_d represents the cut-off frequency and the B_n denotes the elliptic rational function that is utilized to ensure a sharper transition. $|A(\vartheta)|$ represents the amplitude response of the elliptic filter at angular frequency ϑ.

2) Elimination of Power-line Interference

The power-line interference at 50/60 Hz is a disturbing artifact in ECG signal recordings that hampers the analysis of the electrical signal. A Chebyshev Type I filter was used to achieve a sharper transition between the passband and stopband by permitting variations in the passband. The amplitude response is represented by:

$$|A(\vartheta)| = \frac{1}{\sqrt{1+\varepsilon^2 C_n^2\left(\vartheta/\vartheta_d\right)}} \quad (2)$$

where C_n represents the Chebyshev polynomial of order n. This filter successfully removes the power-line interference

(50/60 Hz) without greatly impacting the ECG signal. $C_n(\vartheta)$ represents the n^{th} order Chebyshev polynomial, that ensures equiripple characteristics exclusively in the passband. The stopband exhibits a monotonic decline (with no ripples). This filter offers a sharper roll-off compared to Butterworth filters, although it is not as sharp as the elliptic filter of the same order.

3) Elimination of Electrode Motion Artifacts

The electrode motion artifact is due to flocked electrodes or because of the contact between the dry electrode and skin, making the ECG recording unstable. The proposed technique used an adaptive comb filter, Finite Impulse Response (FIR), to ensure stability. This filter eliminates periodic noise by focusing on its harmonic frequencies. The transfer function is:

$$A(Z) = \frac{1}{M} \sum_{m=0}^{M-1} Z^{-mk} \quad (3)$$

where M represents several harmonics and k is a sampling index. This filter ensures stability because of its linear-phase characteristic, maintaining the fidelity of the ECG signal. $A(Z)$ denotes a transfer function of the comb filter in the Z-domain, determining how the filter handles the frequency components of the input signal. Preserving signal integrity allows for precise analysis of ECG features, such as QRS complexes and P-waves, which are crucial for clinical diagnosis.

4) Z-Score Normalization

Normalization is performed once the ECG signal is denoised to classify the data with the least redundancy, thus reducing duplication and ensuring that only relevant data is included. This method uses z-score normalization to normalize each value in the dataset, so that it has a mean of zero and scales to unit variance. The signal variation in amplitude and scale would be crucial in multi-source datasets, where this phase enhances the performance of ECG segmentation and pattern recognition systems.

B. False Peak Elimination and Segmentation

The preprocessed and normalized signals may contain false peaks that may affect the accuracy of the results. This phase of the model detects and eliminates these unwanted peaks. Feature extraction detects the peaks and is followed by the segmentation process.

1) False Peak Detection and Elimination

R-peak detection is performed by considering the high amplitude and the slope of the wave. P and T peaks are detected by considering the wave time duration, time of occurrence, the magnitudes of the P and T waves, the distance between the peaks, and the mean value of R peak location features, which have a lower primary spectrum. The detection of R, P, and T peaks is performed before the removal of false peaks, as shown in Figure 2.

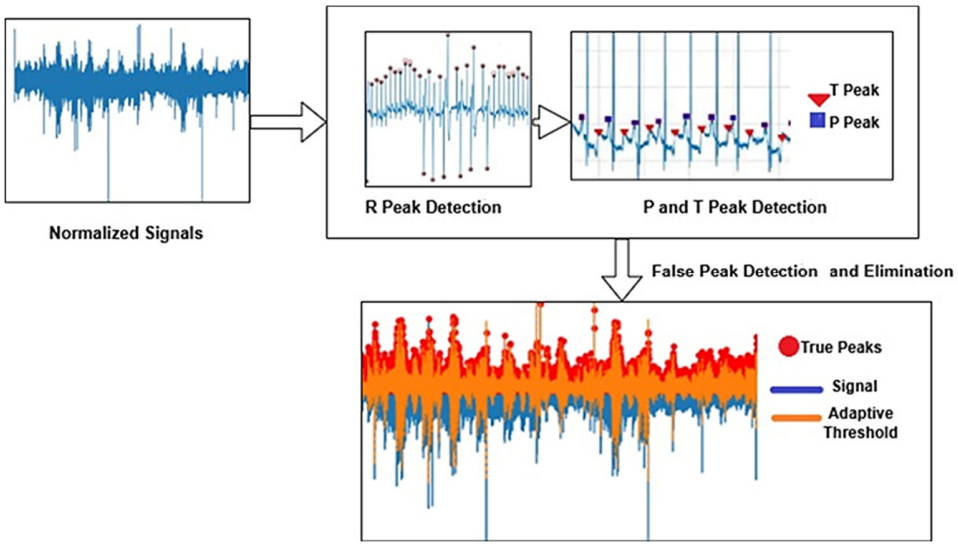

Fig. 2. False peak elimination.

a) R-Peak Detection

The R-peak is crucial for dividing the ECG signal into discrete heartbeats. Its detection relies on two primary attributes: the amplitude of the signal and the slope of the waveform. An R-peak is recognized by locating the maximum amplitude within the ECG signal as:

$$R - Peak = max\ (A_j) \quad (4)$$

where A_j is the amplitude at sample j. Since the R-peak is the point of greatest amplitude, as shown in Figure 2, its identification is the basis for the segmentation process. By determining the R-peak, the QRS complex can be separated, and the signal can be partitioned into distinct heartbeats.

b) P and T Peaks Detection

Once the R-peaks have been identified, the subsequent task is to discern the P-waves (atrial depolarization) and T-waves (ventricular repolarization). The P and T peaks are identified based on a defined set of features:

- The magnitude of the P or T wave.

- The duration of wave time (T_η) for the P or T wave.
- The distance among peaks (e) in relation to the R-peak.
- The average value of the R-peak location characteristics.

The magnitude (N) of the P or T waves is defined as the maximum amplitude obtained over the wave as:

$$N = max(P_{wave}\ or\ T_{wave}) \quad (5)$$

T_η is the time interval during which the P or T wave occurs:

$$T_\eta = Time\ duration\ of\ the\ P\ or\ T\ wave \quad (6)$$

The distance (e) among the peaks helps to estimate the suitable timing relationship between the waves:

$$e = Distance\ between \frac{P}{T} peaks\ and\ the\ R-peak \quad (7)$$

Using these properties, the P and T peaks are obtained based on the timing and the amplitude. The timing-magnitude relation can be described as:

$$\frac{P}{T}\ Peak = \left(Time_{peak}, Amplitude_{peak}\right) \quad (8)$$

where $Time_{peak} \propto T_\eta$.

This equation means that the timing of P or T peak is proportional to the duration of the wave, thus ensuring that the peaks are identified in the appropriate temporal window relative to the R-peaks.

c) False Peak Elimination

Removing false peaks is necessary to only consider the authentic peaks of the ECG signal. This is performed by statistical false peak evaluation and adaptive thresholding. False peak elimination is accomplished by swotting peak-to-peak intervals based on statistical false peak evaluation. The false peak is obliterated using an amplitude axis adaptive threshold and morphological features by statistical evaluation. An adaptive threshold technique alters the threshold according to the mean and standard deviation of the signal's amplitude:

$$T_{adaptive} = \bar{G} + \lambda.\beta_G \quad (9)$$

where $T_{adaptive}$ is the adaptive threshold and λ is a parameter that is adapted according to the dataset. Adaptive thresholding ensures that only the peaks that meet the statistical cut-off are retained, improving the accuracy of the segmentation. In addition to statistical analysis, a morphological evaluation is performed on each peak. The morphology includes the shape, slope, and length of every peak to eliminate the false peaks. Waves that do not match the expected contour or length of standard ECG waveforms are removed.

2) Signal Segmentation

The segmentation process is performed after the step of eliminating false peaks. Now, the signal is separated into different heartbeats. Every section comprises one full QRS complex and T-wave. This ensures correct representation of the individual heartbeats in segmentation, which is crucial for heart rate variability assessment, arrhythmia detection, as well as many other clinical applications. The segmented ECG signal is acquired, where each segment contains one heartbeat.

Using the enhanced linear regression algorithm, false peak removal, and adaptive thresholding, the segmentation method achieves a high level of accuracy. This helps to accurately identify the P, Q, R, S, and T waves, which are important for the subsequent analysis of the ECG signal.

C. Hybrid Feature Extraction and Classification

After the segmentation of ECG signals, a hybrid method, consisting of DL techniques such as Bidirectional Long Short-Term Memory (BI-LSTM) and Neural Basis Expansion Analysis for interpretable Time Series (N-BEATS), is implemented for feature extraction and classification. Figure 3 shows the proposed hybrid framework.

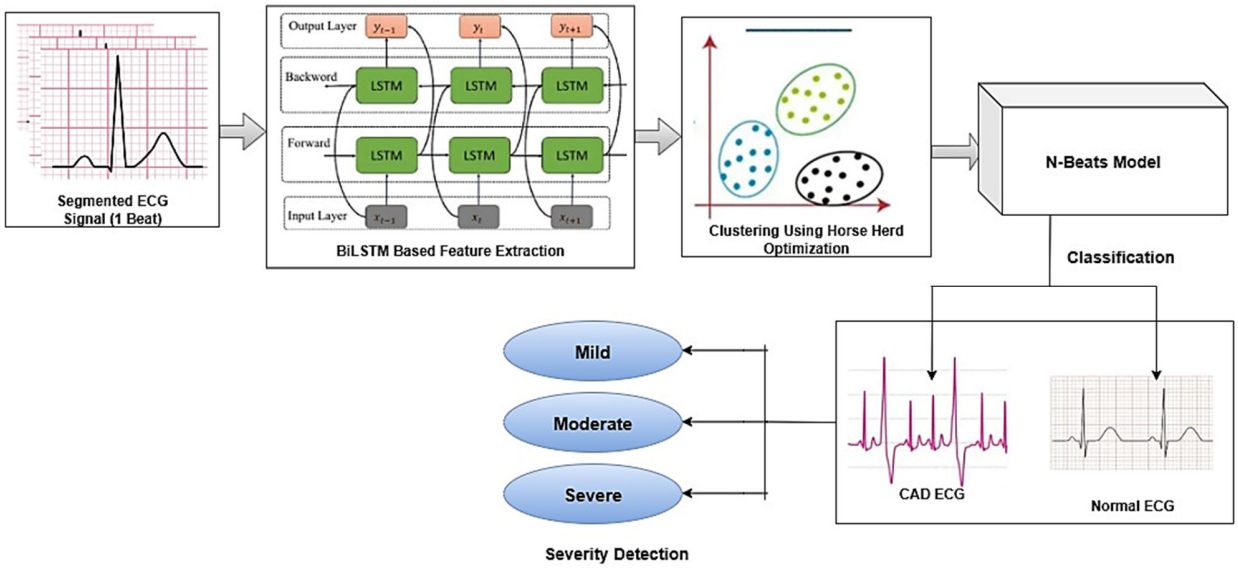

Fig. 3. Hybrid feature extraction and classification framework.

1) Bi-LSTM-Based Feature Extraction

Bi-LSTM is a robust DL architecture tailored to manage sequential data, including ECG signals [13]. This model can grasp temporal dependencies from both previous and subsequent time steps, making it highly effective for time-series applications, such as ECG signal analysis, where context from both sides of the sequence aids in the precise interpretation of the signal. By analyzing the ECG signal in both directions, Bi-LSTM identifies extensive patterns, encompassing both long- and short-range dependencies. The following features are extracted using Bi-LSTM:

- Time-domain features (amplitude-related) are crucial for understanding the fundamental functionalities of the ECG signal. These features help determine irregularities in signals, such as arrhythmias. These are calculated based on the maximum, minimum, mean, and standard deviation of the amplitude.
- Frequency-domain features delineate how the power associated with the ECG signal is distributed over various frequency intervals. Such features are valuable in identifying anomalies such as arrhythmic patterns and harmonics. Frequency-related features are extracted based on mean, standard deviation, skewness, kurtosis, etc.
- Time-frequency domain features inherit information from both the time and frequency domains to offer a more comprehensive consideration of the ECG signal. This is particularly valuable to identify transient phenomena, including variation in the QRS complex or inversion of the T-wave.
- Statistical and morphological features include the detection of QRS duration, P wave onset, T wave slope, etc, that must be incorporated to understand the structure and design of the ECG waveform, which is useful in correct disease classification.

Bi-LSTM plays an important role in the extraction of features from the ECG signal, capturing dependencies over short- and long-term aspects. The data is assessed on both sides, ensuring that temporal patterns within preceding and subsequent contexts are picked up during feature extraction, although mostly related to properties in the time domain, amplitude variance, and statistical properties. These properties would therefore act as inputs into the following stages of the pipeline for classification: N-BEATS and CAD severity detection.

2) Horse Herd Optimization Algorithm (HOA)-based K-means for Feature Selection

To minimize feature dimensionality, the extracted features are clustered using K-means based on the HOA. HOA is a bio-inspired optimization method that mimics the behavior of horse herds [14] and is used in the improvement of traditional clustering algorithms. It functions by modifying the position and velocity of each feature within the cluster through a combination of the current position, the best-known position in the herd (global best), and the best position discovered by the individual horse (local best). This approach maintains a balance between exploration (investigating new regions) and exploitation (focusing on promising regions). The equations for velocity and position used in this method are as follows.

- Velocity:

$$vu_{j+1} = T.vu_j + F_1.U_1.\left(P_{best} - b_j\right) + F_2.U_2.\left(w_{best} - b_j\right) \quad (10)$$

where vu_j is the velocity of feature j, b_j is the position of feature j, T is the inertia weight, F_1, and F_2 are cognitive and social coefficients, U_1, and U_2 are random values between 0 and 1, P_{best} is the local best position (best solution found by feature j), and w_{best} is the global best position (best solution identified by the herd).

- Position:

$$b_{j+1} = b_j + VU_{j+1} \quad (11)$$

where b_{j+1} the updated position of feature j. This update rule enables the algorithm to modify the locations of features to achieve improved clusters, thereby enhancing the clustering process.

As shown in Figure 4, K-means is first employed to group features, allocating each feature to a centroid. However, the efficacy of K-means is improved by refining the centroids through HOA, which improves the locations of the centroids by considering the actions of the horses (features), resulting in more precise clustering. The capacity of HOA to reduce intra-cluster variance results in superior clustering outcomes, ensuring that only relevant features are selected for classification [15].

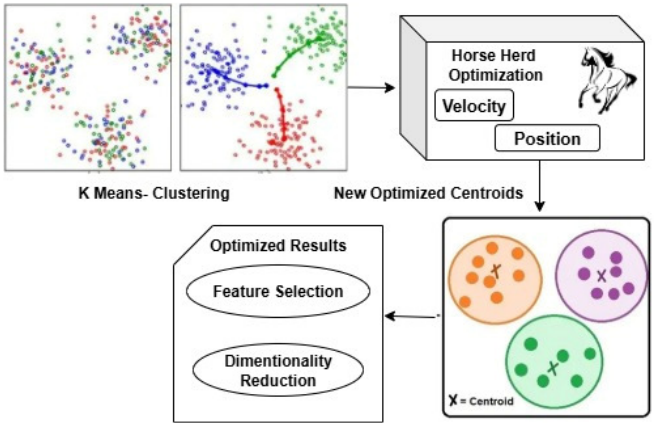

Fig. 4. Integrated K-Means and HOA.

3) N-BEATS for ECG Classification

Classification is performed using N-BEATS, which is a powerful architecture with low complexity that offers higher training speed [16]. N-BEATS is a strong DL framework developed for time-series forecasting and classification. Unlike traditional RNNs, N-BEATS does not rely on a sequential approach, making it more efficient and thus more suitable for ECG classification, especially in diagnosing CAD.

All the features selected using HOA are input to the N-BEATS model. N-BEATS employs three categories of blocks that are intended to capture differing temporal patterns from the ECG data.

- Trend blocks: This block focuses on long-term trends found in the data. It captures consistent, predictable alterations in the ECG signal, such as the overall heart rhythm (e.g., normal sinus rhythm). This block is vital for identifying chronic patterns or gradual changes in heart function.
- Seasonal blocks: This block investigates short-term cyclical patterns. In ECG signals, this might relate to the periodicity of individual heartbeats or cycles. This aids in recognizing rapid changes and deviations from normal patterns, which are essential for identifying arrhythmias or abrupt cardiac incidents.
- Residual blocks: At the core of the N-BEATS architecture are residual blocks, which allow the model to learn more efficiently and avert the vanishing gradient issue that frequently impacts DL models. Residual learning resembles permitting the model to keep some of the original data (input) in every layer, allowing the model to learn from discrepancies (or residuals) instead of merely depending on transformations at each layer.

These fully connected layers produce a classification score that illustrates the probability of the input ECG signal being associated with CAD or not. N-BEATS employs the softmax activation function to convert the raw output (logits) into a probability distribution over various classes. For a binary classification task, such as Normal versus CAD, the softmax function determines the probability of each class in the following manner:

$$R(r = \sigma_u | F) = \frac{k^{V_L}}{\sum_{d=1}^{h} h^{V_L}} \quad (12)$$

where $R(r = \sigma_u | F)$ is the likelihood that the input is part of class σ_u (Normal or CAD), V_L is the unprocessed output (logits) for the class σ_u, h is the count of classes (2 classes: Normal and CAD), r is the response value, and d is the index over the h element. After utilizing the softmax function, the class with the greatest probability is chosen as the predicted label for the input ECG signal.

4) Detection of the Severity Level of CAD

After classification, the severity level of the disease is detected using a signal code for a positive CAD person. The severity level of artery disease is categorized into three classes, namely Mild, Moderate, and Severe, using the Minnesota Code (MC). This method classifies the severity of CAD by analyzing QRS voltage, ST-segment, and T-wave inversion patterns across different ECG leads. Severity classification based on MC is performed as follows:

- Mild CAD: Recognized by the existence of QS pattern and T-wave inversion in Lead II.
- Moderate CAD: Observed when the QS pattern and T-wave inversion manifest in Leads III to V.
- Severe CAD: Identified when the QS pattern and T-wave inversion are detected in more than five leads.

The severity classification can be represented as a conditional function:

$$Severity_{CAD} = \begin{cases} \text{Mild:} & \text{if T} - \text{wave inversion in Lead II and QS on Lead II} \\ \text{Moderate:} & \text{if Lead III} - \text{V's T} - \text{wave is inverted and its QS} \\ \text{Severe:} & \text{If QS exceeds five leads and T} - \text{wave inversion exceeds five leads} \end{cases}$$

where Lead II denotes the lead that displays the first indications of CAD, Leads III-V signify the leads that exhibit more extensive abnormalities, and Severe CAD occurs when abnormalities are observed in a considerable number of leads.

III. EXPERIMENTAL RESULTS

Python 3.11.4 was used to develop the proposed approach.

A. Dataset Used

The proposed model was evaluated on ECG signals from the Fantasia and St. Petersburg [17] dataset available on Physionet. This 12-lead arrhythmia dataset, which is a component of the St. Petersburg Institute of Cardiology Techniques database, provided the CAD ECG signals. Various rhythms (such as ischemia) are included in the recordings, collected from participants aged 18 to 80, with a mean age of 58 years and a roughly equal distribution of genders. This dataset includes reference annotation files with more than 175,000 beat annotations and 75 half-hour recordings taken from 32 Holter records of patients undergoing CAD testing. Fantasia data includes 40 rigorously screened healthy individuals of two different age groups: young adults (21–34 years) and elderly adults (68–85 years). To stay awake, each participant watched Disney's Fantasia for two hours while in a supine position. Signals of St. Petersburg and Fantasia are sampled at 257 and 250 Hz, respectively. Two distinct groups of ECG data, segmented into two seconds (2 s) and five seconds (5 s), were used in the experiment. The signal duration varies for identical patients in both segment sets of data. To ensure that each segment has at least one beat, groups of at least two and five seconds were chosen. The preprocessed signal was normalized to 1000 Hz to provide standardization.

B. Comparative Analysis

The results for PI2DCNN were obtained using a custom-designed parallel-input 2D CNN framework to extract deep recurrence features from ECG signals. These features were classified using an SVM classifier [18]. The results for XGBoost were based on the classification stage of the DLECG-CVD model [19], where the ECG features were extracted using a Deep Belief Network (DBN), optimized with ISSO, and fed into the XGBoost model for CVD diagnosis. The PI2DCNN and XGBoost models achieved 95.96% and 88.2% accuracy on their experimental datasets, respectively. These models achieved 80% and 92% accuracy, respectively, in the dataset used in this study.

These approaches were chosen due to their compatibility. In both models, ECG lead 12 signals were sampled at 1000 Hz, as in this study. In addition, these models are compatible with wavelet features. PI2DCNN performed well on multi-modal

signals with spatial deep features, whereas DBN-XGBoost effectively captured temporal dynamics in large-scale ECG data. These complementary findings support the broader aim of robust CVD detection across data settings. Thus, this section compares the proposed approach to PI2DCNN and XGBoost to evaluate its efficiency using Accuracy, Specificity, Sensitivity, and F1-score, along with a confusion matrix.

1) Accuracy

As the count of epochs increases, models generally learn more effectively, and accuracy improves until it levels off or starts to overfit. Figure 5 and Table II show the accuracy results for the models compared. The numerical results comparing the accuracy of PI2DCNN, XGBoost, and the proposed method over epochs illustrate gradual performance enhancement. At 2 epochs, the accuracy is 20% for PI2DCNN, 25% for XGBoost, and 30% for the proposed method. By 4 epochs, the proposed method shows a substantial advantage with 45% accuracy, in contrast to 29% and 35% for PI2DCNN and XGBoost, respectively. At 6 epochs, the difference increases further, with the proposed method reaching 58% accuracy, surpassing XGBoost (46%) and PI2DCNN (42%). By 8 epochs, the proposed method achieves 86%, significantly exceeding XGBoost (80%) and PI2DCNN (74%). At 10 epochs, the proposed method realizes the highest accuracy at 96%, trailed by XGBoost at 92% and PI2DCNN at 80%, underscoring its exceptional learning ability and efficiency throughout all epochs.

TABLE II. ACCURACY RESULTS

Epochs	Accuracy (%)		
	PI2DCNN	XGBoost	Proposed
2	20	25	30
4	29	35	45
6	42	46	58
8	74	80	86
10	80	92	96

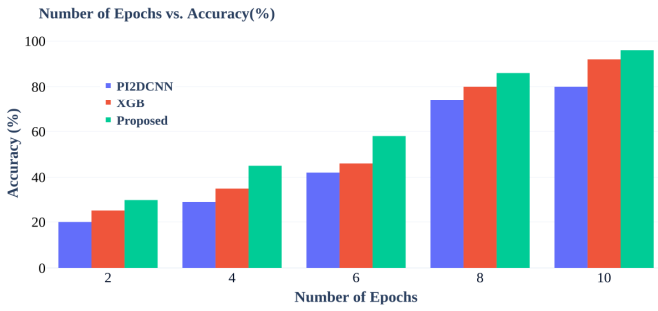

Fig. 5. Accuracy (%) across epochs.

2) Specificity

As epochs increase, the specificity improves as the model becomes more skilled in recognizing negative instances without producing false positives. Figure 6 and Table III illustrate the numerical results of Specificity for PI2DCNN, XGBoost, and the proposed method.

TABLE III. SPECIFICITY RESULTS

Epochs	Specificity		
	PI2DCNN	XGBoost	Proposed
2	0.1	0.2	0.4
4	0.2	0.3	0.5
6	0.4	0.5	0.6
8	0.5	0.7	0.8
10	0.6	0.8	1.0

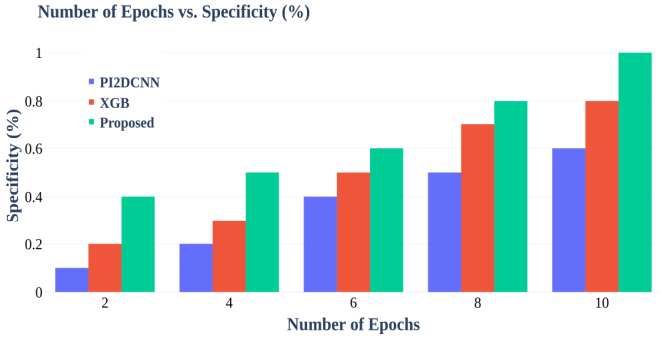

Fig. 6. Specificity (%) across epochs.

At 2 epochs, the specificity is low for all models, beginning at 0.1 for PI2DCNN, 0.2 for XGBoost, and 0.4 for the proposed method. By 4 epochs, the proposed method shows a benefit with a specificity of 0.5, in contrast to 0.2 for PI2DCNN and 0.3 for XGBoost. At 6 epochs, the proposed method continues to lead with 0.6, outperforming XGBoost at 0.5 and PI2DCNN at 0.4. By 8 epochs, the proposed method hits 0.8, while XGBoost reaches 0.7 and PI2DCNN falls behind at 0.5. At 10 epochs, the proposed method achieves flawless specificity (1.0), greatly exceeding XGBoost (0.8) and PI2DCNN (0.6), emphasizing its superior capability to accurately identify negative cases.

3) Sensitivity

As the number of epochs increases, sensitivity increases, as the model becomes more proficient at recognizing positive cases (diseased samples). Figure 7 and Table IV illustrate the numerical results of sensitivity for PI2DCNN, XGBoost, and the proposed method across epochs. At 2 epochs, the sensitivity of the proposed method is already leading at 0.5, in contrast to 0.1 for PI2DCNN and 0.2 for XGBoost. By 4 epochs, the proposed method further boosts to 0.6, surpassing PI2DCNN (0.2) and XGBoost (0.3). At 6 epochs, the sensitivity of the proposed method increases to 0.67, while XGBoost reaches 0.4 and PI2DCNN stays lower at 0.3. By 8 epochs, the proposed method attains 0.7, with XGBoost improving to 0.6 and PI2DCNN at 0.45. At 10 epochs, the proposed method secures perfect sensitivity (1.0), greatly exceeding the other models.

TABLE IV. SENSITIVITY RESULTS

Epochs	Sensitivity		
	PI2DCNN	XGBoost	Proposed
2	0.1	0.2	0.5
4	0.2	0.3	0.6
6	0.3	0.4	0.67
8	0.45	0.6	0.7
10	0.6	0.8	1.0

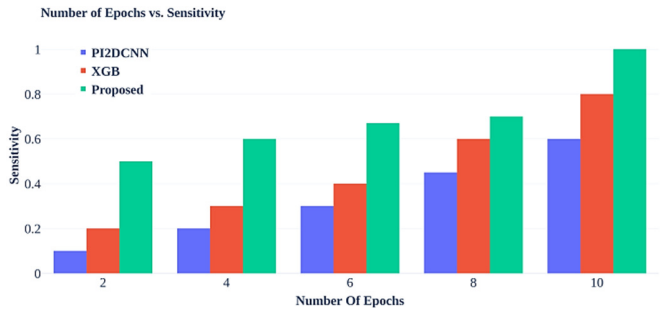

Fig. 7. Sensitivity (%) across epochs.

4) F1-Score

As the count of epochs increases, the F1-score generally increases as the model attains a superior balance between precision and sensitivity. Figure 8 and Table V illustrate the F1-score results for PI2DCNN, XGBoost, and the proposed method over epochs, highlighting the improved performance of the latter in achieving a balance between precision and sensitivity. At 2 epochs, the proposed method begins with an F1-score of 35%, exceeding PI2DCNN (20%) and XGBoost (25%). By 4 epochs, the proposed method reaches 49%, preserving its advantage over PI2DCNN (40%) and XGBoost (45%). At 6 epochs, the proposed method further advances to 56%, in contrast to 54% for XGBoost and 50% for PI2DCNN. By 8 epochs, the F1-score of the proposed method increases to 88%, surpassing XGBoost (84%) and PI2DCNN (80%). At 10 epochs, the proposed method secures a peak F1-score of 95%, showcasing superior performance compared to XGBoost (90%) and PI2DCNN (87%), effectively balancing precision and recall.

TABLE V. F1-SCORE RESULTS

Epochs	F1-score (%)		
	PI2DCNN	XGBoost	Proposed
2	20	25	35
4	40	45	49
6	50	54	56
8	80	84	88
10	87	90	95

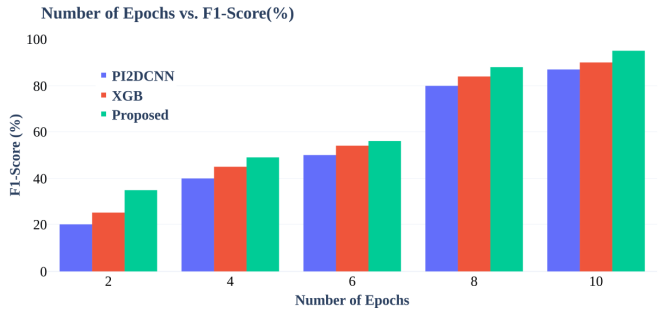

Fig. 8. F1-score across epochs.

5) Confusion Matrices

As the count of epochs increases, confusion matrices are refreshed with enhanced classification results, showcasing improved precision in differentiating positive and negative cases. Figure 9 and Table VI illustrate the numerical results of the confusion matrices. In terms of True Negatives, the proposed method surpasses both PI2DCNN and XGBoost, with a score of 396, in contrast to 320 and 360, respectively. Likewise, regarding False Positives, the proposed method demonstrates an advantage, with 380, while PI2DCNN and XG-Boost present 450 and 410, respectively. When considering False Negatives, the proposed method reveals a decrease as well, reaching 453, compared to 500 for PI2DCNN and 470 for XGBoost. Finally, concerning True Positives, the proposed method leads once more with 311, trailed by 300 for XGBoost and 280 for PI2DCNN. This evaluation emphasizes the superior performance of the proposed method in accurately identifying both True Negatives and True Positives, while effectively reducing False Positives and False Negatives.

TABLE VI. CONFUSION MATRIX RESULTS

	Model		
	PI2DCNN	XGBoost	Proposed
True Negatives	320	360	396
False Positives	450	410	380
False Negatives	500	470	453
True Positives	280	300	311

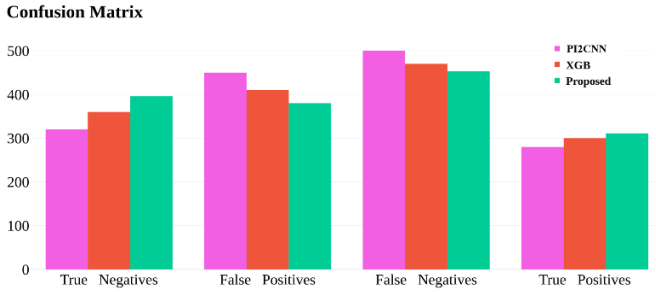

Fig. 9. Confusion matrix results for the tree models.

IV. CONCLUSION

This study presented a novel DL-based framework for CAD detection using ECG signals, addressing signal quality issues by removing various artifacts present in ECG data. The model implemented parameters such as adaptive thresholds on the amplitude axis and morphological features, and selected true amplitude peaks that ensured clean and reliable data for classification. The integration of Bi-LSTM with HOA-based K-means captured complex temporal relationships very well and improved feature extraction. Including N-BEATS helped it improve detection capabilities, thereby adding more robust cardiac event predictions. Finally, CAD severity was determined by monitoring ST depression, ST elevation, and T-wave inversion in various leads of 12-lead ECGs. The experimental results showed that the proposed model achieved 96% accuracy, 1.0 specificity,1.0 sensitivity, and 95% F1-score, outperforming PI2DCNN and XGBoost. Thus, the proposed model is favoured for the detection of CAD at early stages and its severity analysis, and can serve as a useful tool to help clinical professionals quickly validate their diagnosis.

REFERENCES

[1] T. Qi, H. Zhang, H. Zhao, C. Shen, and X. Liu, "Research on ECG Signal Classification Based on Hybrid Residual Network," *Applied Sciences*, vol. 14, no. 23, Dec. 2024, Art. no. 11202, https://doi.org/10.3390/app142311202.

[2] I. D. Mienye and Y. Sun, "Improved Heart Disease Prediction Using Particle Swarm Optimization Based Stacked Sparse Autoencoder," *Electronics*, vol. 10, no. 19, Sep. 2021, Art. no. 2347, https://doi.org/10.3390/electronics10192347.

[3] S. Deivanayagi and P. S. Periasamy, "Computer Aided Coronary Atherosclerosis Plaque Detection and Classification," *Intelligent Automation & Soft Computing*, vol. 34, no. 1, pp. 639–653, 2022, https://doi.org/10.32604/iasc.2022.025632.

[4] H. Zhang *et al.*, "Discrimination of Patients with Varying Degrees of Coronary Artery Stenosis by ECG and PCG Signals Based on Entropy," *Entropy*, vol. 23, no. 7, Jun. 2021, Art. no. 823, https://doi.org/10.3390/e23070823.

[5] L. Yao *et al.*, "Enhanced Automated Diagnosis of Coronary Artery Disease Using Features Extracted From QT Interval Time Series and ST–T Waveform," *IEEE Access*, vol. 8, pp. 129510–129524, 2020, https://doi.org/10.1109/ACCESS.2020.3008965.

[6] L. Xie, Z. Li, Y. Zhou, Y. He, and J. Zhu, "Computational Diagnostic Techniques for Electrocardiogram Signal Analysis," *Sensors*, vol. 20, no. 21, Nov. 2020, Art. no. 6318, https://doi.org/10.3390/s20216318.

[7] A. Darmawahyuni *et al.*, "Deep Learning with a Recurrent Network Structure in the Sequence Modeling of Imbalanced Data for ECG-Rhythm Classifier," *Algorithms*, vol. 12, no. 6, Jun. 2019, Art. no. 118, https://doi.org/10.3390/a12060118.

[8] Z. Ebrahimi, M. Loni, M. Daneshtalab, and A. Gharehbaghi, "A review on deep learning methods for ECG arrhythmia classification," *Expert Systems with Applications: X*, vol. 7, Sep. 2020, Art. no. 100033, https://doi.org/10.1016/j.eswax.2020.100033.

[9] R. Banerjee, A. Ghose, and K. Muthana Mandana, "A Hybrid CNN-LSTM Architecture for Detection of Coronary Artery Disease from ECG," in *2020 International Joint Conference on Neural Networks (IJCNN)*, Glasgow, United Kingdom, Jul. 2020, pp. 1–8, https://doi.org/10.1109/IJCNN48605.2020.9207044.

[10] J. Rymko, M. Solinski, A. Perka, J. Rosinski, and M. Lepek, "Classification of Atrial Fibrillation in Short-term ECG Recordings Using a Machine Learning Approach and Hybrid QRS Detection," presented at the 2017 Computing in Cardiology Conference, Sep. 2017, https://doi.org/10.22489/CinC.2017.337-201.

[11] H. J. Suleiman, I. R. A. Hamid, and O. R. Olaniran, "Smart Health Monitoring for Predicting Heart Disease using IoT-Fog-Cloud Computing Model," *Engineering, Technology & Applied Science Research*, vol. 15, no. 3, pp. 22565–22572, Jun. 2025, https://doi.org/10.48084/etasr.10048.

[12] A. Hernandez-Matamoros, H. Fujita, E. Escamilla-Hernandez, H. Perez-Meana, and M. Nakano-Miyatake, "Recognition of ECG signals using wavelet based on atomic functions," *Biocybernetics and Biomedical Engineering*, vol. 40, no. 2, pp. 803–814, Apr. 2020, https://doi.org/10.1016/j.bbe.2020.02.007.

[13] K. Kaur and G. Bathla, "Deep Learning Approach for Coronary Artery Disease Detection and Severity Analysis Using ECG Signals," in *2024 International Conference on Artificial Intelligence and Quantum Computation-Based Sensor Application (ICAIQSA)*, Nagpur, India, Dec. 2024, pp. 1–6, https://doi.org/10.1109/ICAIQSA64000.2024.10882385.

[14] D. Moldovan, "Horse Optimization Algorithm: A Novel Bio-Inspired Algorithm for Solving Global Optimization Problems," in *Artificial Intelligence and Bioinspired Computational Methods*, vol. 1225, R. Silhavy, Ed. Springer International Publishing, 2020, pp. 195–209.

[15] N. Emami and M. Kuchaki Rafsanjani, "Feature selection strategy based on hybrid horse herd optimization algorithm and perturbation theory: an mRMI approach," *Annals of Operations Research*, Nov. 2024, https://doi.org/10.1007/s10479-024-06389-4.

[16] B. N. Oreshkin, D. Carpov, N. Chapados, and Y. Bengio, "N-BEATS: Neural basis expansion analysis for interpretable time series forecasting." arXiv, Feb. 20, 2020, https://doi.org/10.48550/arXiv.1905.10437.

[17] A. L. Goldberger *et al.*, "PhysioBank, PhysioToolkit, and PhysioNet," *Circulation*, vol. 101, no. 23, pp. e215–e220, Jun. 2000, https://doi.org/10.1161/01.CIR.101.23.e215.

[18] C. Sun *et al.*, "Enhanced CAD Detection Using Novel Multi-Modal Learning: Integration of ECG, PCG, and Coupling Signals," *Bioengineering*, vol. 11, no. 11, Oct. 2024, Art. no. 1093, https://doi.org/10.3390/bioengineering11111093.

[19] O. S. Lih *et al.*, "Comprehensive electrocardiographic diagnosis based on deep learning," *Artificial Intelligence in Medicine*, vol. 103, Mar. 2020, Art. no. 101789, https://doi.org/10.1016/j.artmed.2019.101789.